J Therm Anal Calorim (2011) 104:1145–1151
DOI 10.1007/s10973-011-1346-7

Kinetics of thermo-oxidative degradation of polypropylene/aluminum trihydroxide/organo Fe-montmorillonite nanocomposites

Qinghong Kong · Yuan Hu · Lei Song · Yuwen Tang

Received: 31 August 2010 / Accepted: 12 January 2011 / Published online: 22 February 2011

Abstract In the article, the thermal oxidative degradation kinetics of pure polypropylene/aluminum trihydroxide (PP/ATH) and PP/ATH/organo Fe-montmorillonite (Fe-OMT) nanocomposites were investigated using Kissinger, Friedman and Flynn–Wall–Ozawa methods. The results showed that thermal oxidative degradation of PP/ATH/Fe-OMT nanocomposites to PP/ATH were complex reaction: the whole process of thermal oxidative degradation were composed with the decomposition of ATH, the cracking and charring of the backbone chains of PP, and the oxidative degradation of char, which the curses of energy mutative with the process of thermal oxidative degradation. The control steps were different in each degradation stage. The activation energy was high in the original degradation stage. It was due to the molecular structure and may closely relate with onset temperature. In the intermediate process, the activation energy was low. In the last stage of the degradation, the activation energy was graveled because the carbon may be oxidized. In the whole process of thermal oxidative degradation, the activation energy of PP/ATH/Fe-OMT nanocomposite was higher than that of PP/ATH.

Q. Kong (✉) · Y. Hu (✉) · L. Song
State Key Laboratory of Fire Science, University of Science and Technology of China, Hefei, Anhui 230026, China
e-mail: kongqh@ujs.edu.cn

Y. Hu
e-mail: yuanhu@ustc.edu.cn

Q. Kong · Y. Tang
Jiangsu University Branch Center of State Key Lab of Urban Water Resource and Environment, Jiangsu University, Zhenjiang 212013, China

Keywords Kinetics of thermo-oxidative degradation · Polypropylene · Fe-montmorillonite · Nanocomposite

Introduction

In recent years, the interest in flame-retardants used in polyolefin has been focused on the aluminum trihydroxide (ATH) due to their halogen-free, low toxicity, the absence of dioxins, and low smoke occurring in fire accidents. ATH decomposes and releases water during burning, which reduces the heat and temperature from the substrate [1]. Typically about 60 wt% of filler is required. In addition, very high metal hydroxide concentrations are usually needed to achieve an acceptable degree of flame retardancy and impact strength [2]. The synergistic effect of natural montmorillonite on ATH flame retardant additives in the PP matrix can improve the mechanical property [3, 4]. In a previous report, PP/ATH/Fe-OMT nanocomposites were prepared and characterized [5]. The structure of PP/ATH/Fe-OMT nanocomposites was exfoliated, which were characterized by XRD and TEM. The thermal stability and flame retardancy of PP/ATH/Fe-OMT nanocomposites were better than that of PP/ATH. The synergistic effect of Fe-OMT in flame retardancy of PP/ATH was good and the Fe-OMT showed remarkable catalytic charring effect.

The flammability of polymers is related to their thermo-oxidative degradation behavior at high temperatures. As a consequence, the thermal decomposition details of the materials influence their flame-retardancy to a considerable degree and deserve a deep investigation. The thermal decomposition behavior of materials can be measured by thermogravimetric (TG) analysis. According to the TG data, the kinetic parameters of thermal decomposition of

materials such as apparent activation energy (E_a), pre-exponential factor (A), and apparent reaction order (n) can be calculated using various kinetic models such as Friedman [6], Kissinger [7], Coats-Redfern [8], Flynn–Wall–Ozawa [9, 10], and Horowitz-Metzger [11] methods. Consequently, the thermal decomposition of the flame-retarded polymeric materials can be quantitatively described to reveal the flame-retarding mechanism from the viewpoint of kinetics.

The kinetics of degradation of polymer nanocomposites is also a major concern in the case of polymer with low flammability such as nanocomposites [12–14]. According to those studies mentioned above, the influence of the compositions of Fe-OMT on the kinetic parameters of thermo-oxidative decomposition of the flame-retarded PP material was not reported, that is, the relationship between thermal kinetic parameters of the flame-retarded material with ATH and the corresponding flame retardancy was still not clear. Based on our previous contributions [5], in this article, we studied the kinetics of the thermo-oxidative degradation of the flame-retarded PP/ATH and PP/ATH/Fe-OMT nanocomposites using different kinetic models including Kissinger, Friedman, and Flynn–Wall–Ozawa methods. The kinetic parameters obtained by the above different methods were then compared and meanwhile were connected with the flame-retardancy of the related materials. Kissinger and Flynn–Wall–Ozawa methods were used because they can conveniently obtain the relative activation energy without prior knowledge of the reaction mechanism and the reaction order. Using those methods, we calculated activation energies of thermal degradation of PP/ATH and PP/ATH/Fe-OMT nanocomposite and discuss influence of Fe-OMT on thermal stability and inflaming retarding.

Kinetic methods

The application of dynamic TG methods holds great promise as a tool for unraveling the mechanisms of physical and chemical processes that occur during polymer degradation. The basic assumption of the thermal kinetics is that the Arrhenius equation representative of the reaction rate dependence of the temperature can be applied in the thermal analysis reaction, i.e., for a simple reaction $A_{solid} \rightarrow B_{solid} + C_{gas}$, its reaction rate $d\alpha/dt$ can be written as:

$$\frac{d\alpha}{dt} = kf(\alpha), \tag{1}$$

where $\alpha = (W_0 - W_t)/(W_0 - W_\infty)$ (W_0, W_t, and W_∞ are the initial, actual, and final mass of the sample, respectively, in the TG test), $f(\alpha)$ and k are functions of conversion and temperature, respectively.

Arrhenius equation has the following formula:

$$k = Ae^{-E/RT}, \tag{2}$$

where E is the activation energy, A the pre-exponential factor, and R the gas constant. $f(\alpha)$ depends on the particular decomposition mechanism. The simplest and most frequently used model for $f(\alpha)$in the analysis of TG data is

$$f(\alpha) = (1 - \alpha)^n, \tag{3}$$

where n is the order of the reaction, substitution of Eqs. 2 and 3 in Eq. 1 gives

$$\frac{d\alpha}{dt} = A(1 - \alpha)^n e^{-E/RT}. \tag{4}$$

Kissinger method [12] involves obtaining the temperature values (T_{max}) that occurs at the maximum rate, where $d(d\alpha/dt)/dt$ is zero, differentiation of Eq. 4 with respect to t and setting the resulting expression to zero gives

$$\frac{E\beta}{RT_{max}^2} = An(1 - \alpha_{max})^{n-1} e^{-E/RT_{max}}, \tag{5}$$

where β is heating rate in TG analysis (K min^{-1}) setting as $\beta = dT/dt$.

Kissinger assumes that the product $(1 - \alpha_{max})^{n-1}$ is independent of β and the following expression can be derived:

$$\ln\left(\frac{\beta}{T_{max}^2}\right) = \left\{\ln\frac{AR}{E_a} + \ln\left[n(1 - \alpha_{max})^{n-1}\right]\right\} - \frac{E}{RT_{max}}, \tag{6}$$

where T_{max} corresponds to the temperature at the inflexion point of TG curve and α_{max} is the conversion degree at the inflexion point.

Plot of $\ln(\beta/T_{max}^2)$ against $1/T_{max}$ produces a fitted straight line. According to the slope of this straight line (E/R) the apparent activation energy E can be calculated, i.e., if slope $B = E/R$, then $E = BR$. The advantage of the Kissinger model is that the apparent activation energy can be obtained without the knowledge of any thermal degradation reaction mechanism in advance.

Flynn–Wall–Ozawa method [15], which is essentially the same as that of Flynn and Wall, represents a relatively simple method of determining activation energy directly from mass loss versus temperature data obtained at several heating rates. Equation 4 is integrated using *Doyle's* approximation, and the result of the integration after taking logarithms is:

$$\lg f(\alpha) = \lg\frac{AE}{R} - \lg\beta - 2.315 - 0.4567\frac{E}{RT}, \tag{7}$$

where β, A, E, and T have the known meanings, $f(\alpha)$ is the integral function of conversion. This is one of the integral

methods that can be used to determine the activation energy without knowledge of the reaction order. It is used to determine the activation energy for given values of conversion. The activation energy for different conversion values can be calculated from ln β versus $1/T$ plot.

Friedman method [16] is a differential method, and it directly based on Eq. 4 whose logarithm is

$$\ln\left(\frac{d\alpha}{dt}\right) = \ln\left[\beta\left(\frac{d\alpha}{dt}\right)\right] = \ln A + n\ln(1-\alpha) - \frac{E}{RT}. \quad (8)$$

Using this equation, it is possible to obtain values for E over a wide range of conversions by plotting $\ln(d\alpha/dt)$against $1/T$ for a constant value.

Experimental

Materials

Polypropylene (PP, F401), maleic anhydride grafted PP (PP-*g*-MA), ATH (ATH, OL104/G), Fe-MMT (synthesized as follows: hydrous oxide was prepared by mixing $Na_2SiO_3{\cdot}9H_2O$ with $FeCl_3{\cdot}6H_2O$ and $Zn(COOCH_3)_2{\cdot}2H_2O$ solutions to set the atomic ratio at Si–Fe–Zn = 4–1.7–0.3; the detailed method of synthesis followed previous reports [17]). The cation-exchange capacity (CEC) was 102 m equiv/100 g for Fe-MMT. The Fe-MMT was modified by cetyltrimethyl ammonium bromide (CTAB), and the product was called Fe-OMT.

Preparation of the samples [5]

The PP (the content of maleic anhydride grafted PP was 15% in the PP matrix), additives and desired amounts of Fe-OMT (2 wt%) and ATH were premixed, then extruded at 443 K using a twin-screw extruder (TE-35, JiangShu, China) at 60 rpm for 10 min. The nanocomposites were then compression molded into sheets of 1 mm by a hot press at 443 K and 10 MPa for 10 min, followed by cooling to room temperature.

Characterization

The thermal properties of PP/ATH and PP/ATH/Fe-OMT nanocomposites were investigated by TG analysis with a TA50 Thermoanalyzer instrument. They were heated in the temperature range 293–973 K using heating rates of 5, 10, 15, and 20 K min^{-1}, with a controlled dry air flow of 50 cm^3 min^{-1}. The temperature and the mass scales were calibrated using high-purity standards (indium, nickel, zinc, aluminum, and gold) over a specific range of heating rates with a calibration parameter of their respective melting points.

Results and discussion

In our previous report [5], the structure of PP/ATH/Fe-OMT (2 wt% Fe-OMT) nanocomposite was characterized

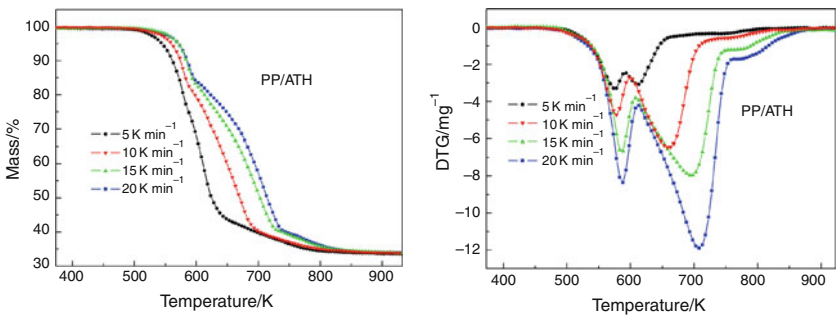

Fig. 1 TG/DTG curves of PP/ATH at different heat rate in air flow

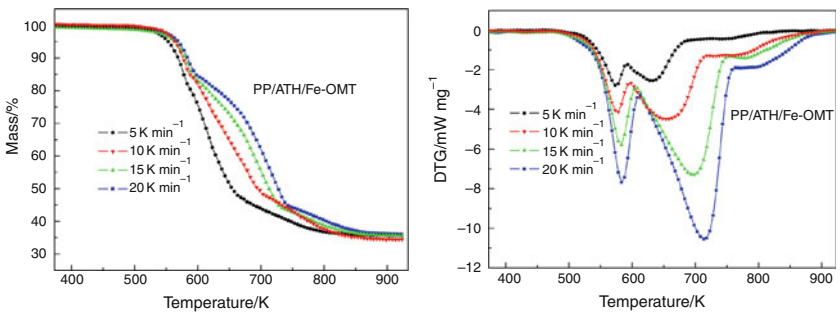

Fig. 2 TG/DTG curves of PP/ATH/Fe-OMT(2 wt% Fe-OMT) at different heat rate in air flow

by the XRD and TEM. The sample was exfoliated nanocomposites and TG was applied to test the thermal properties of nanocomposites. The thermal stability and flame retardancy of PP/ATH/Fe-OMT nanocomposites was better than that of PP/ATH.

Figure 1 shows the TG and DTG curves of the flame-retarded PP materials with ATH. Three thermal decomposition steps in the temperature range 373–923 K. The first step of the decomposition was at 523–573 K which was the decomposition of ATH. At 623–723 K, the major degradation products of PP are olefins. Owing to the protective charred ceramic surface layer and the inner clay layers acting as a sealed microreactor [18], the degradation products were sealed within the PP matrix (allowing more time to interact with the Fe^{3+} catalyst), and dehydrogenation, aromatizing reactions leading to char formation occur. These olefins can activate the hydrogen and dehydrogenation can easily occur in PP in the presence of Fe^{3+} catalyst, generating conjugated dienes which react with an activated double bond and cause cyclization, and the cyclic compounds can further dehydrogenate and aromatize to form char. When the temperature is over 773 K, the char

Table 1 Inflection point temperature of TG curves for different materials at different heating rates

Heating rate/K min^{-1}	$T_{inflection\ point\ 1}$/K		$T_{inflection\ point\ 2}$/K	
	PP/ATH	PP/ATH/Fe-OMT	PP/ATH	PP/ATH/Fe-OMT
5	574.5	576.8	631.2	636.7
10	577.1	580.2	663.3	668.2
15	581.3	584.4	694.6	700.5
20	583.2	586.4	712.3	721.6

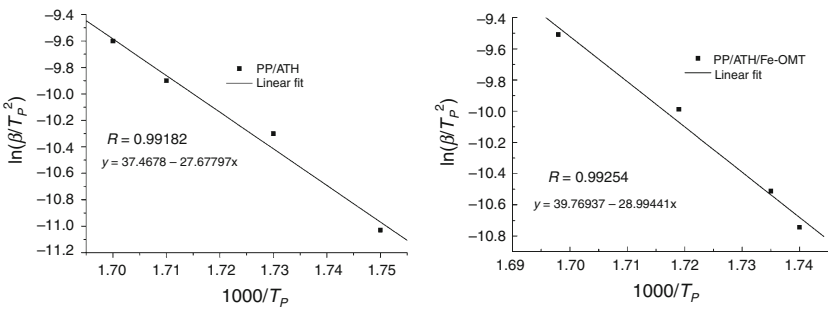

Fig. 3 ln β and $1/T_P$ relation curves of PP/ATH and PP/ATH/Fe-OMT at first course using Kissinger method

Table 2 The activation energies (E_a) obtained using the Kissinger method

Samples	*E_{a1}/KJ/mol	**E_{a2}/KJ/mol	Correlation coefficient (R_1)	Correlation coefficient (R_2)
PP/ATH	230.1	42.7	0.9918	0.9971
PP/ATH/Fe-OMT	241.1	50.5	0.9925	0.9995

* E_{a1} inflection point$_1$ of E_a, ** E_{a2} inflection point$_2$ of E_a

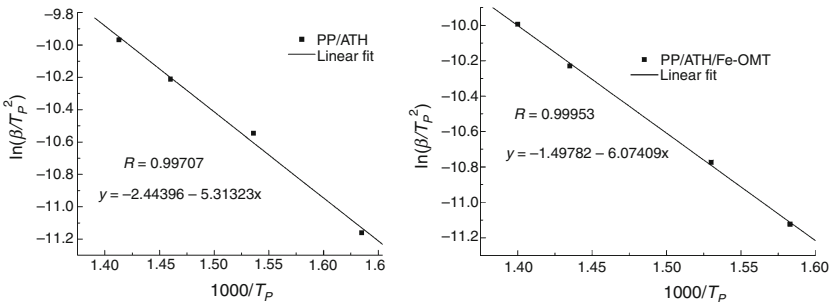

Fig. 4 ln β and $1/T_P$ relation curves of PP/ATH and PP/ATH/Fe-OMT nanocomposite at second course using Kissinger method

Table 3 Kinetics data of PP/ATH and PP/ATH/Fe-OMT nanocomposite obtained by the Friedman method

Conversion α	PP/ATH		PP/ATH/Fe-OMT	
	E_a/KJ/mol	lgA/s	E_a/KJ/mol	lgA/s
0.05	115.22	7.59	194.98	15.11
0.1	135.13	9.48	220.11	17.29
0.2	140.63	9.90	178.70	13.23
0.3	29.09	−0.36	76.45	3.59
0.4	57.88	2.10	63.36	2.47
0.5	51.43	1.63	63.56	2.50
0.6	50.52	1.62	66.87	2.78
0.7	54.87	2.04	73.22	3.27
0.8	75.67	3.63	95.90	4.76
0.9	119.52	6.23	128.83	6.36

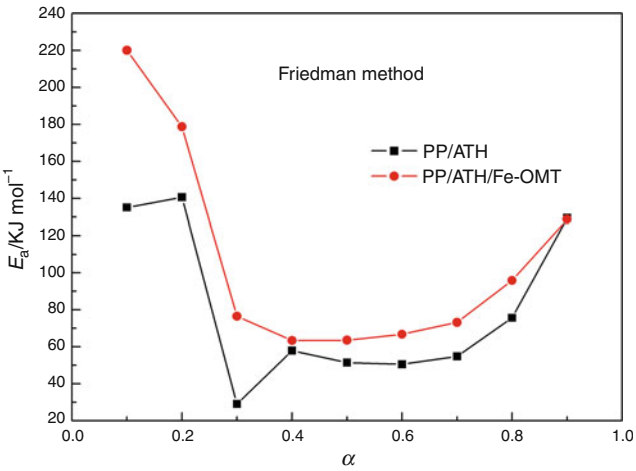

Fig. 5 Thermokinetic curves of PP/ATH and PP/ATH/Fe-OMT nanocomposite under Friedman method

had burnt and many small alveoli were left; the Al_2O_3 acted as framework and formed three-dimensional mesh structure [5].

Kinetics analysis using Kissinger method

The inflection point temperatures of the TG curves of various samples shown in Figs. 1 and 2 are included in Table 1. According to Eq. 7, plots of $\ln\left(\beta/T_{max}^2\right)$ against $1000/T_{max}$ produce the fitted straight lines as shown in Figs. 3 and 4. The obtained slopes of various straight lines were used to calculate the corresponding apparent activation energy (Table 2). As can be seen, the correlation coefficient (R) was very high; the relativity of the various fitted straight lines is very good, showing the feasibility of Kissinger method. According to our previous report [5], thermal stability of PP/ATH/Fe-OMT nanocomposites was better than that of PP/ATH. However, in this study, the nanocomposites with Fe-OMT showed higher mean activation energy than that of PP/ATH. It is observed that incorporation of OMT in the presence of polymer significantly increases activation energy [19], suggesting that the addition of Fe-OMT may change the thermal oxidative degradation behavior of PP/ATH/Fe-OMT nanocomposites [20].

Kinetics analysis using Friedman methods

The Friedman methods were also chosen here. All data are shown in Table 3 and Fig. 5. We can find that the activation energy of PP/ATH/Fe-OMT nanocomposite was higher than that of PP/ATH, which was in accordance with the results obtained from Kissinger method. The span of E_a was large in the whole course of the thermal oxidative degradation. The trend variation of the E_a was coincident

Table 4 Kinetics data of PP/ATH and PP/ATH/Fe-OMT nanocomposites obtained by the Flynn–Wall–Ozawa method

Conversion α	PP/ATH			PP/ATH /Fe-OMT		
	E_a/KJ/mol	lgA/s	Correlation coefficient (R)	E_a/KJ/mol	lgA/s	Correlation coefficient (R)
0.05	114.48	7.51	0.9884	231.96	18.88	0.9878
0.1	131.69	9.16	0.9865	247.36	20.04	0.9936
0.2	159.16	11.71	0.9974	255.36	20.47	0.9896
0.3	91.05	5.27	0.9967	107.09	6.64	0.9863
0.4	65.04	2.82	0.9991	71.36	3.30	0.9767
0.5	55.97	1.98	0.9986	62.95	2.52	0.9923
0.6	52.13	1.66	0.9975	61.63	2.38	0.9981
0.7	50.09	1.51	0.9954	63.70	2.62	0.9984
0.8	52.83	1.77	0.9949	72.11	3.18	0.9993
0.9	99.35	5.35	0.9573	104.12	5.26	0.9988
Mean	87.18	–	–	127.76	–	–

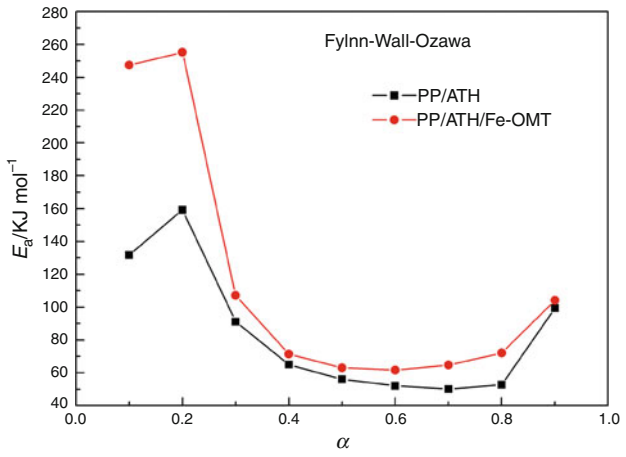

Fig. 6 thermokinetic curves of PP/ATH and PP/ATH/Fe-OMT nanocomposite under Flynn–Wall–Ozawa method

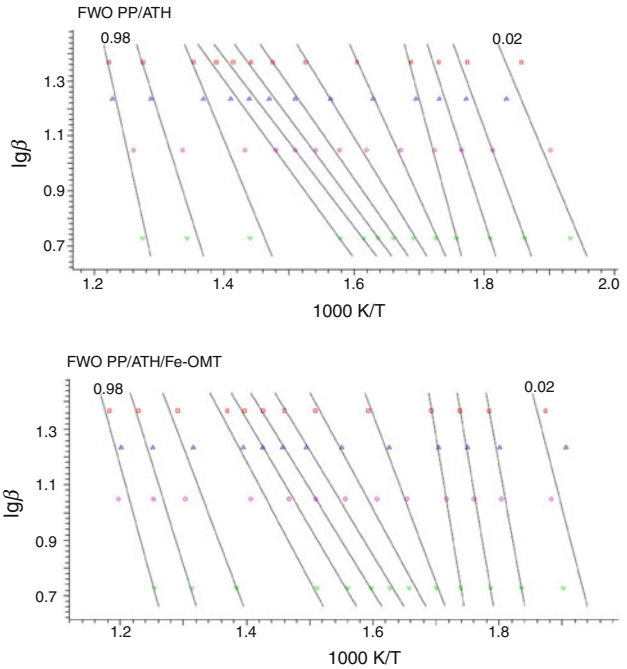

Fig. 7 Ozawa plots of PP/ATH and PP/ATH/Fe-OMT nanocomposite at different conversions

with the curves of TG. The results showed the thermal oxidative degradation of PP/ATH and PP/ATH/Fe-OMT nanocomposites was complex process.

Kinetics analysis using Flynn–Wall–Ozawa method

Flynn–Wall–Ozawa method was used to calculate the activation energy for different conversion values by fitting the plots of ln β versus $1/T$ plot. All data are shown in Table 4; Figs. 6 and 7. From the mean activation energies of PP/ATH and PP/ATH/Fe-OMT nanocomposites obtained by the Flynn–Wall–Ozawa method, it was very easy to gain the same conclusion as those obtained from Kissinger and Friedman methods. The mean activation energies of PP/ATH and PP/ATH/Fe-OMT nanocomposite were 87.18 and 127.76 kJ mol^{-1}, respectively.

All the three methods obtain the conclusion that the introduction of the clay to the PP/ATH increases the activation energy of thermal oxidative degradation. The enhanced thermal stability of the PP/ATH was likely to be associated with this increase. From TEM results, stacked silicate monolayers can be observed, which are randomly distributed in the PP matrix [5]. According to the barrier model [21], these stacked silicate monolayers were barriers. Thus, the degradation rate of a PP/ATH/Fe-OMT nanocomposite should be limited by the diffusion of gaseous decomposition products through the surface barrier of the silicate char [20].

Conclusions

In conclusion, the methods of Kissinger, Friedman, and Ozawa showed their applicability to the kinetic description of thermal oxidative degradation of PP/ATH and PP/ATH/Fe-OMT nanocomposites. The whole process of thermal oxidative degradation was complicated. It was proved that PP/ATH/Fe-OMT nanocomposite had higher activation energies of thermal oxidative degradation than those of PP/ATH. On the other hand, the nanocomposites had higher residues above 723 K than PP/ATH, indicating that Fe-OMT can enhance the charring action of the copolyesters. These results suggested that the nanocomposites show a higher thermal stability than PP/ATH.

Acknowledgements The study was financially supported by the Foundation of State Key Laboratory of Fire Science (No. HZ2010-KF03), Natural Science fund of University in Jiangsu (No. 09KJD620001) and the joint fund of NSFC and CAAC (No. 61079015).

References

1. Ristolainen N, Hippi U, Seppala J, Nykanen A, Ruokolainen J. Properties of polypropylene/aluminum trihydroxide composites containing nanosized organoclay. Poly Eng Sci. 2005;45(12): 1568–75.
2. Rothon R. The emergence of magnesium hydroxide as a fire retardant additive. In: The Plastic and Rubber Institute, editor. Flame Retardants 1990 Conference. London: Elsevier; 1990.
3. Tang T, Chen X, Chen H, Meng X, Jiang Z, Bi W. Catalyzing carbonization of polypropylene itself by supported nickel catalyst during combustion of polypropylene/clay nanocomposite for improving fire retardancy. Chem Mater. 2005;17:2799–802.
4. Gilman JW, Jackson CL, Morgan AB, Jr RH, Manias E, Giannelis EP et al., Flammability properties of polymer-layered-silicate nanocomposites polypropylene and polystyrene nanocomposites. Chem Mater. 2000; 12:1866–1873.

5. Kong QH, Hu Y, Song L, Yi CW. Synergistic flammability and thermal stability of polypropylene/aluminum trihydroxide/Fe-montmorillonite nanocomposites. Polym Adv Technol. 2009;20: 404–9.
6. Opfermann J. Kinetic analysis using multivariate non-linear regression. I. Basic concepts. J Therm Anal Calorim. 2000;60: 641–58.
7. Mamleev V, Bourbigot S, Le Bras M, Duquesne S, Sestak J. Modelling of nonisothermal kinetics in thermogravimetry. Phys Chem Chem Phys. 2000;2(20):4708–16.
8. Mamleev V, Bourbigot S, Le Bras M, Lefevbre J. Three model-free methods for calculation of activation energy in TG. J Therm Anal Calorim. 2004;78(3):1009–27.
9. Opfermann JR, Kaisersberger E, Flammersheim HJ. Model-free analysis of thermoanalytical data-advantages and limitations. Thermochim Acta. 2002;391(1–2):117–27.
10. Rose N, Le Bras M, Bourbigot S, Delobel R, Costes B. Comprehensive study of the oxidative degradation of an epoxy resin using the degradation front model. Polym Degrad Stab. 1996; 54(2–3):355–60.
11. Flynn JH. Polymer degradation. Handbook of thermal analysis and calorimetry, Amsterdam: Elsevier; 2002; 3: 587–651.
12. Kissinger HE. Reaction kinetics in differential thermal analysis. Anal Chem. 1957;29:1702–6.
13. Lomakin SM, Dubnikova IL, Shchegolikhin AN, Zaikov GE, Kozlowski R, Kim GM, Michler GH. Thermal degradation and combustion behavior of the polyethylene/clay nanocomposite prepared by melt intercalation. J Therm Anal Calorim. 2008; 94(3):719–26.
14. Abate L, Blanco I, Bottino FA, Di Pasquale G, Fabbri E, Orestano A, Pollicino A. Kinetic study of the thermal degradation of PS/MMT nanocomposites prepared with imidazolium surfactants. J Therm Anal Calorim. 2008;91(3):681–6.
15. Ozawa T. A new method of analyzing thermogravimetric data. Bull Chem Soc Japan. 1965;38(1):1881–6.
16. Friedman HL. Kinetics of thermal degradation of char-forming plastics from thermogravimetry: application to phenolic plastic. J Polym Sci Part C. 1964;6:183–95.
17. Kong QH, Hu Y, Song L, Wang YL, Chen ZY, Wan WC. Influence of Fe-MMT on crosslinking and thermal degradation in silicone rubber/clay nanocomposites. Polym Adv Technol. 2006; 17(6): 463–467.
18. Zhu J, Uhl FM, Morgan AB, Wilkie CA. Studies on the mechanism by which the formation of nanocomposites enhances thermal stability. Chem Mater. 2001; 13(12): 4649–4654.
19. Goodarzi V, Jafari SH, Khonakdar HA, Monemian SA, Mortazavi M. An assessment of the role of morphology in thermal/thermo-oxidative degradation mechanism of PP/EVA/clay nanocomposites. Polym Degrad Stab. 2010;95(5):859–69.
20. Wang DY, Wang YZ, Wang JS, Chen DQ, Zhou Q, Yang B, Li WY. Thermal oxidative degradation behaviours of flame-retardant copolyesters containing phosphorous linked pendent group/montmorillonite nanocomposites. Polym Degrad Stab. 2005;87: 171–6.
21. Vyazovkin S, Dranca I, Fan XW, Advincula R. Kinetics of the thermal and thermo-oxidative degradation of a polystyrene/clay nanocomposite. Macromol Rapid Comm. 2004;25(3):498–503.